Moisture-dependent morphing tunes the dispersal of dandelion diaspores

Madeleine Seale[1-4], Oleksandr Zhdanov[5], Cathal Cummins[1,3,6], Erika Kroll[1], Mike Blatt[7], Hossein Zare-Behtash[5], Angela Busse[5], Enrico Mastropaolo[2], Ignazio Maria Viola[6], and Naomi Nakayama[1,3,8] *

[1]School of Biological Sciences, Institute of Molecular Plant Sciences, University of Edinburgh, EH9 3BF, UK
[2]School of Engineering, Institute for Integrated Micro and Nano Systems, University of Edinburgh, EH9 3FF, UK
[3]Centre for Synthetic and Systems Biology, University of Edinburgh, EH9 3BF, UK
[4]School of Energy, Geosciences, Infrastructure and Environment, Institute of Life and Earth Sciences, Heriot-Watt University, EH14 4AS, UK
[5]School of Engineering, University of Glasgow, G12 8QQ, UK
[6]School of Engineering, Institute for Energy Systems, University of Edinburgh, EH9 3DW, UK
[7]Laboratory of Plant Physiology and Biophysics, Bower Building, University of Glasgow, G12 8QQ, UK
[8]Centre for Science at Extreme Conditions, University of Edinburgh, EH9 3FD, UK
*Corresponding author.

Long distance dispersal (LDD) is considered particularly important for plant range expansion (1). Such events are rare, however, and for wind-dispersed species updrafts or extreme weather events are required (1–3). Despite the importance of LDD for plant population dynamics, dispersing long distances is risky to the survival of individual seeds and the majority of seeds disperse short distances. The extent to which most wind dispersed plants can manipulate dispersal ranges of individual seeds is debatable as wind speeds are generally more variable than seed traits (4–9). Here, we present a dynamic mechanism by which dandelion (*Taraxacum officinale*) seeds can regulate their dispersal in response to environmental conditions. We used time lapse imaging to observe shape changes in dandelion pappi. We also analysed diaspore fluid mechanics in two wind tunnels and used particle image velocimetry (PIV) to understand flight characteristics of the morphing structure. We have found that by changing the shape of the pappus when wet, detachment from the parent plant is greatly reduced and seed falling velocities are increased with a significant change in velocity deficit behind the seed. We suggest that this may be a form of informed dispersal maintaining LDD in dry conditions, while spatiotemporally directing short-range dispersal toward beneficial wetter environments.

wind dispersal | biological fluid mechanics | abscission bias | dandelion | Asteraceae

Correspondence: *naomi.nakayama@ed.ac.uk*

Results and Discussion. Wind-dispersed plants are thought to have little control over dispersal distances of individual seeds. This is because variation in wind velocity is generally much greater than intraspecific variation in plant traits (2, 4–8, 10). On average, however, seed falling velocities are important predictors of dispersal distances between species (11–16) arising from differences in seed mass and flight-aiding appendages, such as wings or hairs.

Dandelions are one of the most familiar examples of a wind-dispersed plant. Composite inflorescences produce 100-300 diaspores in a spherical seed-head (capitulum) (Fig. 1a). The dandelion diaspore (referred to hereafter as seed), consists of an achene (fruit) attached to a pappus of around 100 filaments (17) (Fig. 1c). We previously described the mechanism that confers the pappus with its remarkable flight capacity (17).
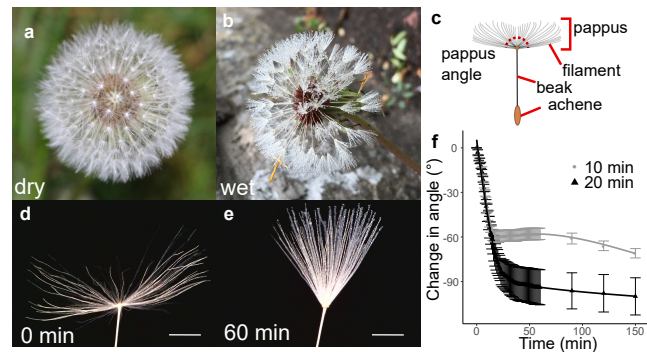

Fig. 1. **Dandelion pappi close when wet. a** image of a dry dandelion capitulum, **b** image of a wet dandelion capitulum, **c** schematic of a dandelion diaspore (seed) indicating features, **d** image of dry dandelion pappus, scale bar = 5 mm. **e** image of dandelion pappus after 1 hour in moisture chamber with a 20 min humidifier treatment, scale bar = 5 mm. **f** time course of change in pappus angle between outermost filaments with 10 or 20 min humidifier treatment, n = 10 and n = 12 samples for 10 and 20 min treatments respectively, error bars are s.e.m.

A separated vortex ring forms behind the pappus due to high porosity of the pappus combined with precise spacing of the filaments, limiting air flow through the pappus.

The dandelion pappus's geometry is not fixed, but changes shape when wet (Fig. 1) (18) (as cited in (19)). Analysis of μCT scans of dry dandelion pappi indicated that, at a 2 mm radius from the centre of the pappus, filaments are, on average, approximately horizontal (Fig. S1a, median = 3.8° from horizontal). Initially, pappus opening occurs when the capitulum first opens and seeds dry out. This phenomenon is clearly reversible, as wetting re-closes the pappus (Fig. 1). To understand closure dynamics, we imaged dandelion seeds in an enclosed chamber with moisture added via an ultrasonic humidifier for 10 or 20 minutes. Images were acquired during humidifier treatment and after for a total of 150 minutes (Fig. 1d-f).

For both conditions, the pappus angle (the angle between outermost filaments, see Fig. 1c) rapidly decreased (4.0 ± 1.4 °/min) during moisture treatments and for 5-15 minutes after moisture addition ceased. An almost steady state was reached at a change in angle of approximately 60° and 90° for the 10 and 20 minute treatments respectively (Fig. 1f). The ultrasonic humidifier releases small droplets of liquid

water into the chamber meaning that relative humidity (RH) reaches 100% within the first few minutes. To test the effect of RH below 100%, we placed samples in a chamber with large dishes of saturated salt solutions, which maintain constant, defined RH levels when in an airtight chamber (20). Samples were imaged at 0 hours and 10 hours, when RH had long reached equilibrium. At a low RH (39.8%), no change in angle was observed while at 71.8% and 87.0%, modest angles changes of around 10° and 24° respectively were observed (Fig. S1b). Together, these results indicate that the dandelion pappus remains open over a wide range of humidity but partially closes at high RH, and rapidly closes when fully wet.

We predicted that the pappus shape change would modify seed flight and indeed found a strong effect on the falling velocity of the seed (Fig. 2a-b). Falling velocity was measured via drop tests for dry seeds, and seeds that had been wet for 1 hour by the humidifier. A decrease in pappus angle of around 100-150°, associated with wetting, resulted in double to triple the falling velocity Fig. 2a-b). The change in projected pappus area that occurs when the pappus closes is likely to be largely responsible for changes in falling velocity and, indeed, a negative linear relationship was observed (Fig. S2a).

To understand how changing the pappus shape affects the drag force on the dandelion seed, we calculated the drag coefficient (C_D) and Reynolds numbers (Re) from our drop test data. C_D is a nondimensionalized indication of the drag force on an object for a given projected area, while Re is a nondimensionalized indication of the fluid regime based on fluid characteristics, speed and size of the object (see Methods). For dry seeds we examined C_D and Re alongside data from weighted/clipped seeds from (17) Fig. 2c). The Re-C_D relationship for dry seeds from this study is comparable to that of weighted/clipped seeds, with higher Re associated with rapidly decreasing C_D before reaching a plateau. The wet seeds with closed pappi, however, exhibit a different C_D-Re relationship with substantially lower C_D for a given Re compared to dry (weighted) seeds with open pappi Fig. 2c). Closing the pappus therefore has two simultaneous effects: Re is increased by the increase in falling velocity and the drag force per unit of projected pappus area is decreased relative to a hypothetical seed with an open pappus of the same projected area. This indicates that adopting a more conical shape is associated with shifting to a different range of the C_D-Re parameter space.

We wanted to understand how wetting impacted on the separated vortex ring (SVR) that forms behind the pappus (17). We examined stationary dandelion pappi in dry and wet states in a vertical wind tunnel (Fig. 2d). Flow visualisation confirmed the presence of the SVR in both open and more closed pappi (Fig. 2e-f). Using a high-speed camera recording at 125 frames per second, we performed particle image velocimetry (PIV) (21) to spatially resolve the varying velocity of air in the region behind the pappus. Our PIV analysis was able to detect the expected features of the SVR (Fig. 2d, S22b,c) (17).

In the region of space directly behind the centre of the pappus, the minimum streamwise flow velocity (minimum u_z) was quantified (Fig. S2d). The magnitude of the minimum u_z showed no clear relationship with the pappus angle in these experimental conditions (Fig. S2d). However, the location of minimum u_z did correlate with pappus angle (Fig. 2g, S2e). At more open pappus angles, the position of minimum u_z moved further downstream of the pappus ($z\ position/dry\ pappus\ diameter = 0.24 + 0.0039 \times pappus\ angle\ (°)$, $p = 0.001$, $R^2 = 0.34$, Fig. 2g).

We used this linear relationship to predict the position of the centre of the vortex and obtain less noisy velocity profiles in the r direction (e.g. Fig. S2b). The integral of a fixed central region of this velocity profile illustrates the magnitude of the velocity deficit in the wake of the pappus, with smaller values indicating a greater velocity deficit. This deficit is closely related to the drag force on the pappus. A significant negative relationship ($p < 0.001$, $R^2 = 0.65$) was observed between pappus angle and the velocity integral (Fig. 2i) indicating that a greater volume of air is moving more slowly behind the pappus when it is more open. Furthermore, the size of the vortex significantly changes with altered pappus angle. The nominal length (see Methods) of the vortex was markedly reduced at smaller pappus angles (Fig. 2h, $p < 0.001$, $R^2 = 0.46$).

The nature of the SVR behind circular disks is strongly affected by the porosity of the disk and Re (17), which is a function of the projected area and flow velocity. In our case, closing the pappus has several effects on the geometry. Firstly, the projected area exposed to the flow reduces (Fig. S2a), secondly, porosity of the pappus reduces as filaments move closer together (Fig. 2j), and thirdly, the shape of the pappus becomes less disk-like and more cone-like. We have observed that the combination of these effects alters the fluid mechanics around the pappus by reducing the size, velocity deficit and changing the positioning of the vortex (Fig. 2e-i).

The velocity deficit behind porous disks is associated with negative pressure (22). In our experiments, streamwise flow velocity was kept constant throughout giving Re = 133-197 across different pappus angles. A larger vortex with a greater velocity deficit may therefore increase the magnitude of the negative pressure, enhancing drag on the pappus.

As drag and falling velocity are strongly affected by pappus closure, we expected this would impact on dispersal distances. To examine the effects of dandelion pappus closure in the context of the wider environment, we modelled the effects of varying falling velocity on dispersal distances in various weather conditions. We obtained hourly meteorological data for 30 years of the summer/autumn period (April to November, when dandelion seeds are typically dispersed) at 5 locations in the UK. Wind speeds at the height of a dandelion capitulum were inferred as described by (23) assuming a release height of 35 cm from the ground (24). For Edinburgh, the hourly wind speeds varied around a mean at measurement height (10 m above ground) of 4.0 m/s (Fig. 3a) and at dandelion height of 0.7 m/s.

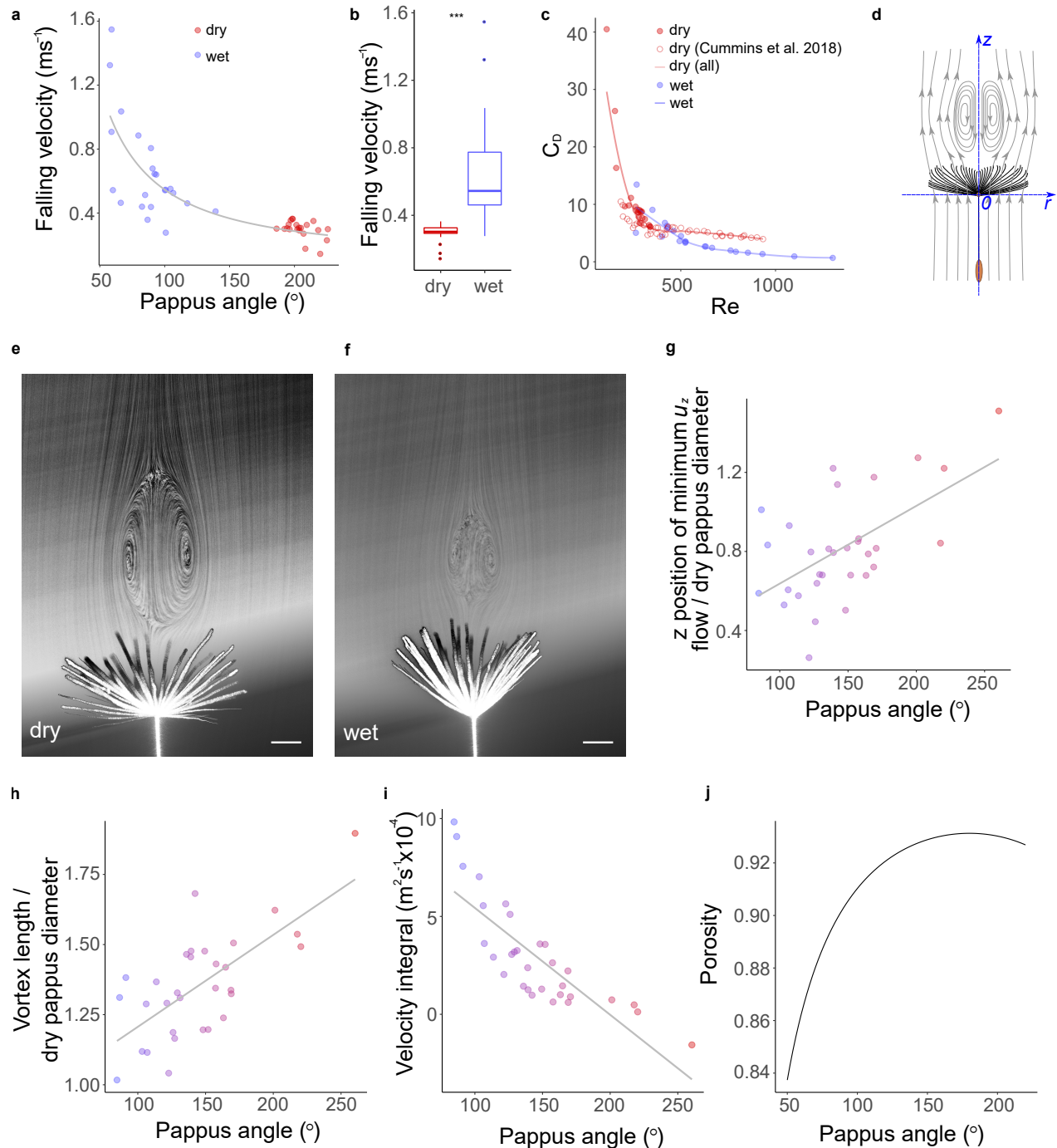We used the hourly wind speed data as an input into the well-

Seale *et al.* | Moisture-dependent morphing in dandelions

Fig. 2. Seed flight and fluid dynamics are modified by pappus closure. a falling velocity at varying pappus angles, n = 20. **b** falling velocity of seeds before and after wetting for 1 hour in moisture chamber, asterisks indicate statistically significant difference at p < 0.0001, n = 20 (same data as a), **c** relationship between Reynolds number (Re) and drag coefficient (C_D) for dry and wet samples, open red circles indicate data from weighted/clipped dry seeds from (17), n = 10 seeds, filled circles are same data as a, n = 20 seeds, **d** schematic illustrating axes and direction of flow for PIV analysis, **e** flow visualisation of dandelion fruit with open pappus, contrast adjusted to illustrate vortex more clearly, scale bar = 2 mm, **f** flow visualisation of dandelion fruit with a partially closed pappus, contrast adjusted to illustrate vortex more clearly, scale bar = 2 mm, **g** distance of the region of minimum u_z flow from the pappus centre at varying pappus angle, position is normalised by the diameter of the pappus when dry, n = 12 seeds, **h** vortex length normalised by the diameter of the pappus when dry at varying pappus angles, n = 12 seeds, **i** integral of the u_z velocity profile at the calculated position of maximal reverse flow, n = 12 seeds, **j** estimated porosity at varying pappus angles.

described analytical WALD model that predicts seed dispersal distances based on wind speeds (25), with varying falling velocities according to weather conditions (Fig. 3b-d, S3e-p). At high RH, when dandelion pappi are more likely to be closed, wind speeds are typically low (Fig. 3a, S3a-e). As dandelion pappi can partially close at RH > 70% (Fig. S1b) and field-measured RH > 90% is a good proxy for wetness on plant surfaces (26), we used RH = 90% as a cut-off point between dry and wet conditions.

For seeds with pappi that are always maximally open (falling velocity = 0.3 m/s) and disperse in any condition, the median dispersal distance for Edinburgh is 0.67 m (Fig. 3b). If dispersal in wet conditions is associated with a higher seed falling velocity (open/closed (dry/wet)), median dispersal is reduced to 0.60 m (Fig. 3b). In such conditions, long distance dispersal, defined here as the furthest 1% of dispersal distances, is also slightly reduced (median = 4.11 m vs 3.78 m) compared to open-pappus dispersers (Fig. 3d). Dispersing only in dry conditions with the pappus open has a modest effect on median dispersal (median = 0.76 m) compared to seeds that disperse in all weathers (Fig. 3b). Similarly, for dry-only dispersers, there is a small positive effect on LDD (Fig. 3d) (median = 4.11 m vs 3.90 m). These patterns were similar in all geographical locations examined (Fig. 3b,d, S3e-h,m-p).

From our earlier observations, we initially predicted that pappus closure would act to alter dispersal distances. However, our modelling showed only modest changes to both median dispersal distances and LDD. Despite similar probability distributions of dispersal distances for seeds with or without dynamic pappus closure (Fig. 3b,d), the suitability of locations for those seeds may not be equal. Considering only the dispersal of seeds in wet conditions, dispersal distances of seeds with a closed pappus are much more likely to remain close to the parent where it is wet, compared to those dispersing with an open pappus (Fig. 3c). Seeds that disperse in wet conditions will not travel far (Fig. 3c). This might be particularly relevant to plants growing in very wet microclimates that cannot be captured with typical meteorological measurements.

Although there appears to be a limited impact of variable falling velocity on dispersal distances, pappus closure may have more effect on detachment from the parent plant. The wind force required to detach seeds would be greater when the pappus is closed and more streamlined. Correlations between detachment, higher wind speeds and low relative humidity have been observed for various anemochorous species during daily (27) and seasonal (16, 28, 29) humidity cycles, indicating dry seed release may be generally beneficial. Wright *et al.* (16) observed a positive impact of dry-season seed release on Tabebuia seed dispersal, though Treep *et al.* (24) found no effect of moisture-based detachment biases on modelled dispersal distances of various Asteraceae species.

Field observations previously showed that dandelion seed detachment correlated with hourly wind speeds at 20 m height of 2-6 m/s (0.31 - 0.94 m/s at dandelion height). We analysed the proportion of hours in which detachment might occur in
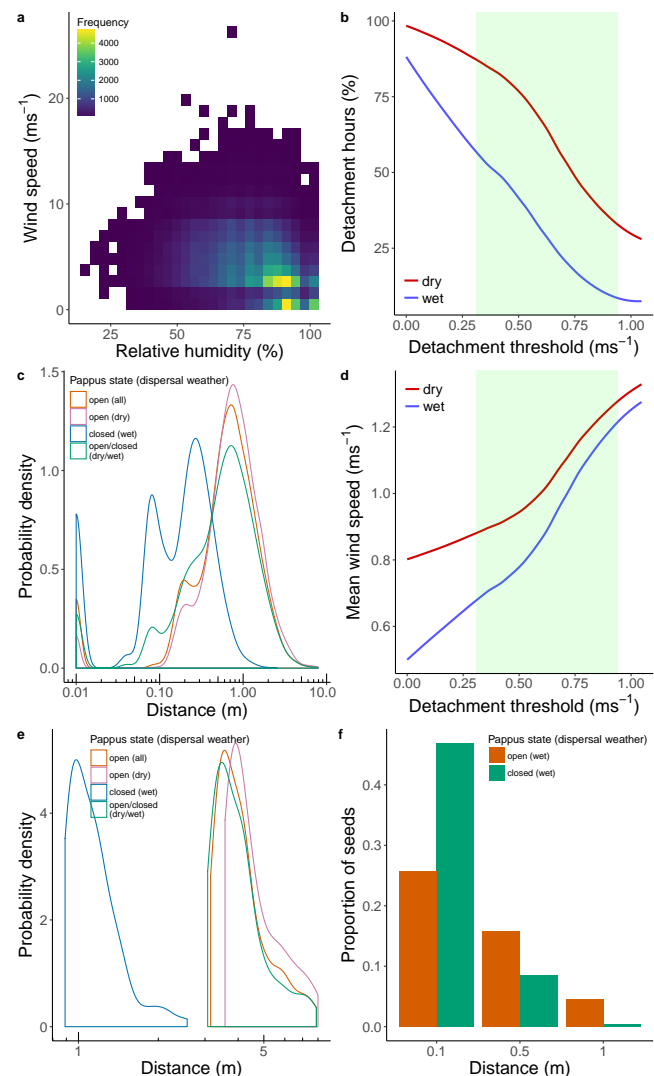

Fig. 3. Change in pappus angle modifies flight according to meteorological conditions. a relationship between relative humidity and wind speed in Edinburgh, UK, **b** probability density distribution of predicted dispersal distances for seeds with open or closed pappi and for different weather conditions, 'dry' indicates that only wind speeds observations for which humidity was less than 90% were used, 'wet' indicates the inverse, and 'dry/wet' corresponds to varying falling velocities depending on the humidity, **c** proportion of seeds travelling short distances in wet conditions with the pappus open or pappus closed, **d** probability density distribution of predicted dispersal distances of furthest 1% of seeds in same conditions as **b**, **e** percentage of hours in which detachment could occur for dry conditions (red line, relative humidity less than 90%) or wet conditions (blue line, relative humidity greater than 90%) at varying detachment thresholds, green shaded area indicates the observed detachment range from (24) corrected to dandelion height, **f** mean wind speed at dandelion height above detachment threshold for dry conditions (red line) and wet conditions (blue line) at varying detachment thresholds.

dry and wet conditions for all our tested locations. For dry Edinburgh conditions, a detachment threshold of 0.31 m/s at dandelion height (the lower end of the observed range in (24)) results in 87% of dry hours in which hourly wind speeds are above threshold (Fig. 3e), and a mean hourly wind speed for these hours of 0.9 m/s (Fig. 3f). Assuming detachment occurs less easily in wet conditions, a threshold at the upper end of the observed range (0.94 m/s), results in hourly wind speeds above threshold in just 9.7% of wet hours (Fig. 3e) with a mean hourly wind speed of 1.2 m/s (Fig. 3f). As the overall mean wind speed at RH ≥ 90% is 0.44 m/s (consid-

Seale *et al.* | Moisture-dependent morphing in dandelions

erably lower than in dry periods), this indicates that reduced seed detachment when wet may generally prevent dispersal initiation during times with low wind speeds. These trends were consistent across all locations examined except Exeter, which showed slight differences in wind speeds (Fig S3q-x).

Force thresholds on detachment are an important mechanism by which plants can bias timing of dispersal in favour of increased wind speeds (9, 24, 27, 30–35). This is thought to promote LDD for some species (9, 33, 35). Since our meteorological analysis indicated that the likelihood of seed detachment may be strongly affected by humidity, we tested detachment experimentally in a wind tunnel. We placed capitula in a wind tunnel (Fig. 4a) and assessed the number of seeds detaching at varying wind speeds (Fig 4).

Hydrating samples for one hour significantly ($p < 0.001$, $\chi^2 = 1088$, $df = 1$) reduced detachment for the range of wind speeds tested (Fig 4d). In flow with 1.7% turbulent intensity, 59% of dry seeds remained attached by the time the highest wind speed was reached (10 m/s), compared to 93% of wet seeds (Fig. 4d). A similar decrease in detachment for wet samples was also observed in flows at higher turbulent intensities (9.1%) (Fig. S4). In flows with higher turbulent intensity, there was also a significant ($p < 0.001$, $\chi^2 = 297$, $df = 1$) increase in the detachment of dry seeds compared to lower turbulent intensity flow (Fig. 4e). These data indicate a powerful impact of hydration and air flow on the initiation of dispersal, consistent with detachment data for thistles (34, 36, 37). The turbulent intensities used here are comparable to that in some natural conditions (38), though turbulence in the atmospheric boundary layer exhibits enormous variability, with values as high as 400% reported (39).

While these wind speeds are well above the hourly wind speed thresholds observed in the field, lab conditions involve several simplifications, and instantaneous wind speeds vary considerably around hourly averages. Typically, maximum gust speeds in the environment are 1.2 to 2 times the hourly mean (38, 40). Most plant tissues exhibit viscoelastic and hydration-dependent mechanical properties (41, 42), meaning that yield stress (and thus detachment) might be affected by the rate of force applied. Gusts may therefore be disproportionately important for detachment, which are difficult to generate in a standard wind tunnel, and have been demonstrated to successfully detach dandelion seeds (31). This is supported by the increased detachment that occurs in more turbulent conditions (Fig. 4e). Additionally, a history of high wind speeds may facilitate detachment by weakening the connection point of a seed.

Dispersal models usually only consider the distance from the source. Distance from a parent is a useful proxy for a favourable environment in terms of reducing resource competition, but is not the only factor affecting the suitability of a location. Soil moisture levels are temporally and spatially variable (43, 44), more so than other environmental variables such as light and temperature (45) meaning that optimal germination locations and times may vary considerably with changing weather. Adult dandelion plants occupy
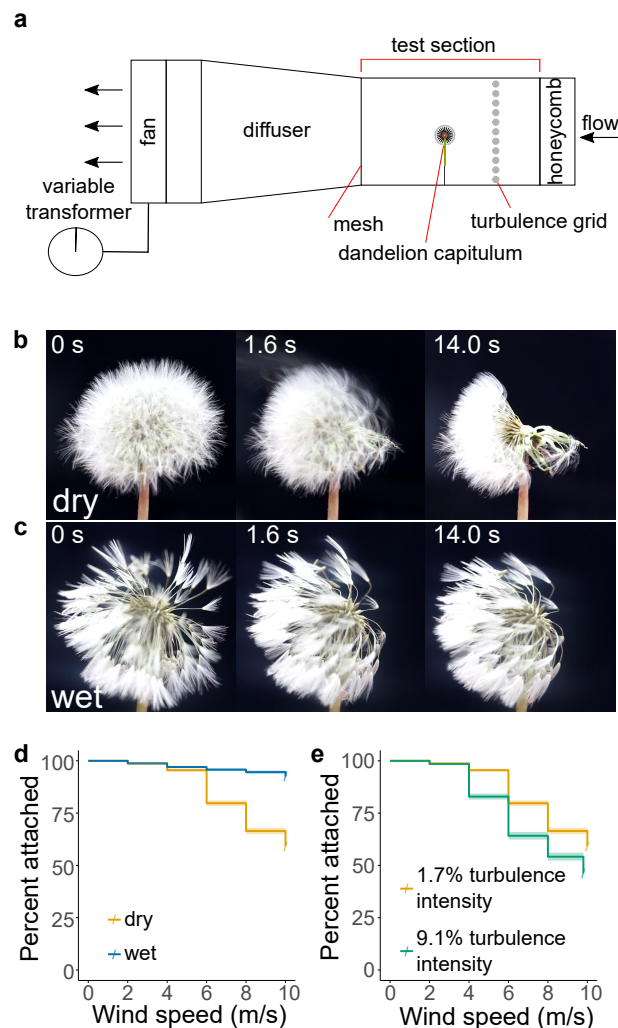

Fig. 4. **Detachment of seeds from capitula. a** diagram of experimental setup, **b** snapshots of detachment at 8 m/s wind speed for a dry capitulum, **c** snapshots of detachment at 8 m/s wind speed for a wet capitulum, **d** survival plot of percentage of fruits attached to capitula at varying wind speeds for 1.7% turbulent intensity flow in dry and wet conditions, tested 3 days after opening of capitula, n = 21 capitula per treatment corresponding to 3736 and 3652 seeds for dry and wet conditions respectively, shading around lines indicates s.e.m. **e** survival plot of percentage of fruits attached to capitula at varying wind speeds for dry conditions with turbulent intensities of 1.7% and 9.1%, tested 3 days after opening of capitula, (data for 1.7% turbulent intensity are the same as for dry capitula in panel **d**), n = 20 capitula for the 9.1% turbulent intensity treatment corresponding to 2677 seeds, shading around lines indicates s.e.m.

a quite variable hydrological niche indicating that they tolerate an environment with appreciable frequencies of both flooding and drought (46). Seedlings though, are more sensitive to hydrological fluctuations but germinate quite well in high moisture conditions (47). One motivation for germinating when more wet, may be that flooding can inhibit establishment of competing species providing a more open area for germination and growth (48). As a result, dispersal to a location with sufficient water availability may be important. Dynamic changes to pappus morphology may thus be a form of informed dispersal, in which dispersal is directed according to environmental characteristics (49). This has previously been demonstrated over longer timescales for developmental

adaptation of heteromorphic seeds to environmental stresses (50).

Dynamic changes in detachment capacity and falling velocity for the same individual or species have not yet been combined in dispersal modelling. This is despite the fact that many (possibly most) pappus-bearing Asteraceae appear able to hygroscopically modify their pappus angle (18) (as cited in (19)) as well as pappus-bearing seeds from diverse flowering plant families in which the mechanism likely evolved independently (51). Future insight into the extent to which dispersal is modified in wet conditions in the field will be crucial to disentangle the effects of detachment and falling velocity. Our meteorological data and modelling use hourly wind speeds, which demonstrate general trends, but do not capture effects of localised eddies and thermal updrafts, which are likely to be important for dispersal (3). An understanding of localised airflow in and around herbal canopies in differing humidity conditions will be necessary to fully understand patterns of seed release.

We propose that closing the pappus in response to moisture may maintain dispersal distances in dry conditions by biasing seed release in favour of greater wind speeds, while retaining some seeds in wet conditions to aid germination. This is at least partially mediated via changes to fluid mechanical properties around individual seeds and entire seed heads. Increasing our understanding of environmental impacts on seed dispersal will help predict the effects on vegetation of changing climatic conditions and extreme weather events.

ACKNOWLEDGEMENTS
We thank Alex Twyford, Jonathan Silvertown and Tomasz Zielinksi for critical reading of the manuscript. We also thank Kazan Federal University Library for providing access to the 1894 manuscript by Taliev (18).

COMPETING FINANCIAL INTERESTS
The authors declare no competing financial interests.

Bibliography

1. Ran Nathan, Frank M Schurr, Orr Spiegel, Ofer Steinitz, Ana Trakhtenbrot, and Asaf Tsoar. Mechanisms of long-distance seed dispersal. *Trends in Ecology and Evolution*, 23:638–647, 2008. doi: 10.1016/j.tree.2008.08.003.

2. Ran Nathan, Gabriel G. Katul, Henry S. Horn, Suvi M. Thomas, Ram Oren, Roni Avissar, Stephen W. Pacala, and Simon A Levin. Mechanisms of long-distance dispersal of seeds by wind. *Nature*, 418:409–413, 2002. doi: 10.1038/nature00930.1.

3. O Tackenberg, P Poschlod, and S Kahmen. Dandelion seed dispersal: the horizontal wind speed does not matter for long-distance dispersal - it is updraft! *Plant Biology*, 5:451–454, 2008. doi: 10.1055/s-2003-44789.

4. Henry S Horn, Ran Nathan, and Sarah R Kaplan. Long-distance dispersal of tree seeds by wind. *Ecological Research*, 16:877–885, 2001.

5. Ran Nathan, Urial N. Safriel, and Imanuel Noy-Mier. Field validation and sensitivity analysis of a mechanistic model for tree seed dispersal by wind. *Ecology*, 82:374–388, 2001.

6. Carol K Augspurger and Susan E Franson. Wind dispersal of artificial fruits varying in mass, area, and morphology. *Ecology*, 68:27–42, 1987.

7. Carol K Augspurger, Susan E Franson, Katherine C Cushman, and Helene C Muller-Landau. Intraspecific variation in seed dispersal of a Neotropical tree and its relationship to fruit and tree traits. *Ecology and Evolution*, 6:1128–1142, 2016. doi: 10.1002/ece3.1905.

8. D. F. Greene and E. A. Johnson. Can the variation in samara mass and terminal velocity on an individual plant affect the distribution of dispersal distances? *The American Naturalist*, 139:825–838, 1992.

9. Sally E Thompson and Gabriel G. Katul. Implications of nonrandom seed abscission and global stilling for migration of wind-dispersed plant species. *Global Change Biology*, 19: 1720–1735, 2013. doi: 10.1111/gcb.12173.

10. Olav Skarpaas, Edward J. Silverman, Eelke Jongejans, and Katriona Shea. Are the best dispersers the best colonizers? Seed mass, dispersal and establishment in Carduus thistles. *Evolutionary Ecology*, 25:155–169, 2011. doi: 10.1007/s10682-010-9391-4.

11. Paul Caplat, Ran Nathan, and Yvonne M Buckley. Seed terminal velocity, wind turbulence, and demography drive the spread of an invasive tree in an analytical model. *Ecology*, 93: 368–377, 2012. doi: 10.1890/11-0820.1.

12. Felix Heydel, Sarah Cunze, Markus Bernhardt-Römermann, and Oliver Tackenberg. Long-distance seed dispersal by wind : disentangling the effects of species traits , vegetation

13. Helene C Muller-Landau, S Joseph Wright, Osvaldo Calderón, Richard Condit, and Stephen P Hubbell. Interspecific variation in primary seed dispersal in a tropical forest. *Journal of Ecology*, 96:653–667, 2008. doi: 10.1111/j.1365-2745.2008.01399.x.

14. Merel B. Soons, Gerrit W. Heil, R Nathan, and Gabriel G. Katul. Determinants of long-distance seed dispersal by wind in grasslands. *Ecology*, 85:3056–3068, 2004.

15. Oliver Tackenberg, Peter Poschlod, and Susanne Bonn. Assessment of wind dispersal potential in plant species. *Ecological Monographs*, 73:191–205, 2003. doi: 10.1890/0012-9615(2003)073[0191:AOWDPI]2.0.CO;2.

16. S Joseph Wright, Ana Trakhtenbrot, Gil Bohrer, Matteo Detto, Gabriel G Katul, Nir Horvitz, Helene C Muller-Landau, Frank A Jones, and Ran Nathan. Understanding strategies for seed dispersal by wind under contrasting atmospheric conditions. *Proceedings of the National Academy of Sciences of the United States of America*, 105:19084–19089, 2008. doi: 10.1073/pnas.0802697105.

17. Cathal Cummins, Madeleine Seale, Alice Macente, Daniele Certini, Enrico Mastropaolo, Ignazio Maria Viola, and Naomi Nakayama. A separated vortex ring underlies the flight of the dandelion. *Nature*, 562:414–418, 2018. doi: doi.org/10.1038/s41586-018-0604-2.

18. V Taliev. On the hygroscopic tissue of the Compositae pappus. [in Russian]. *Proceedings of the Society of Naturalists at the Imperial University of Kazan*, 27:1–38, 1894.

19. W. Rothert. On the hygroscopic tissue of the Compositae pappus [in German]. *Botanisches Zentralblatt*, 63:320–324, 1895.

20. A. Wexler and S. Hasegawa. Relative humidity-temperature relationships of some saturated salt solutions in the temperature range 0° to 50° C. *Journal of Research of the National Bureau of Standards*, 53:19–26, 1954. doi: 10.6028/jres.053.003.

21. Markus Raffel, Christian E. Willert, Fulvio Scarano, Christian J. Kähler, Steve T. Wereley, and Jürgen Kompenhans. *Particle Image Velocimetry A Practical Guide*. Springer, Cham, 3 edition, 2018. doi: 10.1007/978-3-319-68852-7.

22. Cathal Cummins, Ignazio Maria Viola, Enrico Mastropaolo, and Naomi Nakayama. The effect of permeability on the flow past permeable disks at low Reynolds numbers. *Physics of Fluids*, 29:97103, 2017. doi: 10.1063/1.5001342.

23. Olav Skarpaas and Katriona Shea. Dispersal patterns, dispersal mechanisms, and invasion wave speeds for invasive thistles. *The American Naturalist*, 170:421–430, 2007. doi: 10.1086/519854.

24. Jelle Treep, Monique de Jager, Leandra S Kuiper, Gabriel G Katul, and Merel B Soons. Costs and benefits of non-random seed release for long-distance dispersal in wind-dispersed plant species. *Oikos*, 127:1330–1343, 2018. doi: 10.1111/oik.04430.

25. G G Katul, A Porporato, R Nathan, M Siqueira, M B Soons, D Poggi, H S Horn, and S A Levin. Mechanistic analytical models for long-distance seed dispersal by wind. *The American Naturalist*, 166:368–381, 2005.

26. Paulo C Sentelhas, Anna Dalla Marta, Simone Orlandini, Eduardo A Santos, Terry J Gillespie, and Mark L Gleason. Suitability of relative humidity as an estimator of leaf wetness duration. *Agricultural and Forest Meteorology*, 148:392–400, 2008. doi: 10.1016/j.agrformet.2007.09.011.

27. D F Greene, M Quesada, and C Calogeropoulos. Dispersal of seeds by the tropical sea breeze. *Ecology*, 89:118–125, 2008.

28. Felix Heydel and Oliver Tackenberg. How are the phenologies of ripening and seed release affected by species' ecology and evolution? *Oikos*, 126:738–747, 2017. doi: 10.1111/oik.03442.

29. Ran Nathan, Uriel N Safriel, Imanuel Noy-meir, and Gabriel Schiller. Seed release without fire in Pinus halepensis, a Mediterranean serotinous wind-dispersed tree. *Journal of Ecology*, 87:659–669, 1999.

30. Gil Bohrer, Gabriel G Katul, Ran Nathan, Robert L Walko, and Roni Avissar. Effects of canopy heterogeneity, seed abscission and inertia on wind-driven dispersal kernels of tree seeds. *Journal of Ecology*, 96:569–580, 2008. doi: 10.1111/j.1365-2745.2008.01368.x.

31. David F Greene. The role of abscission in long-distance seed dispersal by the wind. *Ecology*, 86:3105–3110, 2005.

32. David Savage, Catherine P Borger, and Michael Renton. Orientation and speed of wind gusts causing abscission of wind-dispersed seeds influences dispersal distance. *Functional Ecology*, 28:973–981, 2014. doi: 10.1111/1365-2435.12234.

33. Peter Schippers and Eelke Jongejans. Release thresholds strongly determine the range of seed dispersal by wind. *Ecological Modelling*, 185:93–103, 2005. doi: 10.1016/j.ecolmodel.2004.11.018.

34. Olav Skarpaas, Richard Auhl, and Katriona Shea. Environmental variability and the initiation of dispersal: turbulence strongly increases seed release. *Proceedings of the Royal Society B*, 273:751–756, 2006. doi: 10.1098/rspb.2005.3366.

35. Merel B Soons and James M Bullock. Non-random seed abscission, long-distance wind dispersal and plant migration rates. *Journal of Ecology*, 96:581–590, 2008. doi: 10.1111/j.1365-2745.2007.0.

36. Eelke Jongejans, Nicholas M Pedatella, Katriona Shea, Olav Skarpaas, and Richard Auhl. Seed release by invasive thistles: the impact of plant and environmental factors. *Proceedings of the Royal Society B*, 274:2457–2464, 2007. doi: 10.1098/rspb.2007.0190.

37. Katherine M Marchetto, Eelke Jongejans, Katriona Shea, and Richard Auhl. Water loss from flower heads predicts seed release in two invasive thistles. *Plant Ecology & Diversity*, 5:57–65, 2012. doi: 10.1080/17550874.2012.667841.

38. Farzin Ghanadi, Matthew Emes, Jeremy Yu, Maziar Arjomandi, and Richard Kelso. Investigation of the atmospheric boundary layer characteristics on gust factor for the calculation of wind load. *AIP Conference Proceedings*, 1850:130002, 2017. doi: 10.1063/1.4984496.

39. J D Wilson, D P Ward, G W Thurtell, and G E Kidd. Understanding strategies for seed dispersal by wind under contrasting atmospheric conditions. *Boundary-Layer Meteorology*, 24:495–519, 1982. doi: 10.1007/BF00120736.

40. Francis K Davis and Herman Newstein. The variation of gust factors with mean wind speed and with height. *Journal of Applied Meteorology*, 7:372–378, 1968.

41. M A Ha, D C Apperley, and M C Jarvis. Molecular Rigidity in Dry and Hydrated Onion Cell Walls. *Plant Physiology*, 115:593 – 598, 1997.

42. Lothar Köhler and Hanns-Christof Spatz. Micromechanics of plant tissues beyond the linear-

Seale *et al.* | Moisture-dependent morphing in dandelions

elastic range. *Planta*, 215:33–40, 2002. doi: 10.1007/s00425-001-0718-9.

43. Jared K Entin, Alan Robock, Konstantin Y Vinnikov, Steven E Hollinger, Suxia Liu, and A Namkhai. Temporal and spatial scales of observed soil moisture variations in the extra-tropics. *Journal of Geophysical Research: Atmospheres*, 105:11865–11877, 2000. doi: 10.1029/2000JD900051.

44. Konstantin Y Vinnikov, Alan Robock, Nina A Speranskaya, and C Adam Schlosser. Scales of temporal and spatial variability of midlatitude soil moisture. *Journal of Geophysical Research: Atmospheres*, 101:7163–7174, 1996. doi: 10.1029/95JD02753.

45. Jonathan Silvertown, Yoseph Araya, and David Gowing. Hydrological niches in terrestrial plant communities: a review. *Journal of Ecology*, 103:93–108, 2014. doi: 10.1111/1365-2745.12332.

46. Jonathan Silvertown, Mike E Dodd, David J G Gowing, and J Owen Mountford. Hydrologically defined niches reveal a basis for species richness in plant communities. *Nature*, 400: 61, 1999.

47. Nathan S Boyd and Rene C Van Acker. The Effects of Depth and Fluctuating Soil Moisture on the Emergence of Eight Annual and Six Perennial Plant Species. *Weed Science*, 51: 725–730, 2003.

48. P J Grubb. The maintenance of specie-richness in plant communities: the importance of the regeneration niche. *Biological Reviews*, 52:107–145, 1977. doi: 10.1111/j.1469-185X.1977.tb01347.x.

49. Jean Clobert, Jean-François Le Galliard, Julien Cote, Sandrine Meylan, and Manuel Massot. Informed dispersal, heterogeneity in animal dispersal syndromes and the dynamics of spatially structured populations. *Ecology Letters*, 12:197–209, 2009. doi: 10.1111/j.1461-0248.2008.01267.x.

50. Carlos Martorell and Marcela Martínez-López. Informed dispersal in plants: Heterosperma pinnatum (Asteraceae) adjusts its dispersal mode to escape from competition and water stress. *Oikos*, 123:225–231, 2014. doi: 10.1111/j.1600-0706.2013.00715.x.

51. Abraham Fahn and Ella Werker. *Anatomical Mechanisms of Seed Dispersal*. Academic Press, Inc., 1972. ISBN 9780323150675. doi: 10.1016/B978-0-12-424301-9.50010-3.

Methods.

Plant growth and samples. *Taraxacum officinale* samples were collected and grown as described previously (1). All samples were the progeny of plants grown in the greenhouse for 2 generations originating from the same individual. As this subspecies reproduces apomictically, all seeds used were considered to be genetically identical. For detachment assays, dandelions were grown in the greenhouse and stems with capitula harvested once the inflorescence had closed but before the infructescance had opened. 15 ml tubes were filled with water and covered by a piece of parafilm with a small hole in and the stems of samples placed through the hole. These samples were then placed in a greenhouse (ambient conditions except for day length, which is artificially extended with electric lighting to ensure at least 16 hours of daylight) to allow the infructescance (capitulum) to open.

Pappus angle measurements. Source data and analysis of 3D micro-tomography CT scans were identical to (1). Angles of each filament from the horizontal axis was calculated at a 2 mm radius from the centre of the pappus, with the beak aligned to the vertical axis. For all other pappus angle measurements, the angle was measured from 2D microscope or camera images. The pappus was aligned perpendicular to the objective/lens and pappus angle measured as the angle between the outermost filaments.

Moisture chamber imaging. The moisture chamber consisted of a 70 L airtight plastic box (Solent Plastics, UK). A hole was made in the box to pass cables through and the space around sealed with silicone sealant. Two USB microscopes (Maozua, USB001) were positioned horizontally to image dandelion seed samples, which were fixed in place by embedding in plasticine or individual pieces of foil shaped around the achene. An ultrasonic humidifier (Bottle Caps) was filled with distilled water and placed next to the dandelion samples. Samples were imaged each minute for the duration of the experiment.

Falling velocity assays. Drop tests were carried out as previously described (1). Samples were tested in two batches (n = 10 and n = 11). First, all seeds were weighed together to obtain the mean weight per sample. Each sample was dropped 3 times and video recorded with a DSLR camera (Canon). Samples were then imaged in the moisture chamber while still dry. The humidifier was switched on for 1 hour and samples re-imaged. Seeds were removed from the chamber one by one and dropped 3 times before placing back inside the humid chamber to prevent further drying. After all samples were dropped, all were weighed together again. The mean increase in weight after wetting was 70 µg, which is unlikely to have a significant effect on falling velocity. Falling velocity was determined from the video frames using a particle detection script as previously described (1).

Calculated variables. The projected area was calculated according to the pappus angle, assuming 100 straight, non-overlapping filaments of length 7.41 mm and diameter 16 µm. Porosity was calculated as the ratio of empty space between filaments (i.e. 1 – the projected area) to the total area of the circle that would enclose the projected area. The Reynolds number is defined as $Re = uD/\nu$, where u is the flow velocity (generally the falling velocity), D is the characteristic length scale (in our case, this is the diameter of the pappus assuming filament length of 7.41 mm) and ν is the kinematic viscosity of the fluid at 20°C. The drag coefficient was calculated as follows:

$$C_D = mg/(0.5\rho u^2 A)$$

where ρ is the density of air, A is the projected area of the disk, taking into account porosity, and g is gravitational acceleration. Additionally, m is the mass of the seed, for which an average measured value of 0.614 mg was used for all samples.

Particle image velocimetry (PIV) and flow visualisation. Samples were fixed in place inside a vertical wind tunnel for flow visualisation and PIV as previously described (1). Long exposure images were obtained using a Canon DSLR camera (EOS 70D). The raw experimental images were processed to distinguish the region of interest (i.e. the SVR) from the reflective pappus. To do this, we applied a digital graduated neutral density filter using the "Curves" contrast adjust tool and the "Blend" tool within the open source software GNU Image Manipulation Program (GIMP version 2.8.22). For PIV, videos were obtained with a high-speed camera (Fastcam Photron SA1.1) shooting at 125 frames per second fitted with a macro lens (Tamron). Air flow velocity was 0.207 m/s throughout. 100 frames of each video were analysed in PIVlab (Matlab) (2) using single pass direct cross correlation with a window size of 128 pixels (corresponding to 3.88 mm) and a step size of 64 pixels. Data were filtered by excluding vectors of more than 2 standard deviations and a normalized median filter (3) with a minimum normalization level (ϵ) of 0.1 pixels and a detection threshold of 3. Vectors were interpolated where missing and the mean vector field of all 50 pairs of images was calculated. Noisy rows of data from the images were excluded from further analysis by removing the first row of the image (row size defined by the window size), which was always noisy, and identifying other noisy rows by fitting an autoregressive integrated moving average (ARIMA) model (R package 'tsoutliers') to the streamwise velocity (u_z) profile across the r direction of the image. u_z profiles with outliers were considered noisy. A z portion of the image with no more than one consecutive noisy row was considered to form the vortex region and was used for further analysis. Analysis was also limited in the r direction by excluding regions of data that fell outside of the limits of the dandelion pappus width. The co-ordinates of the central point of the pappus and the pappus angle were measured from images. The pappus limits were calculated assuming the pappus formed a triangular shape with filaments that were 7.41 mm long (1). The point of minimal u_z flow was determined by finding the co-ordinates of the minimal flow in the z direction at the r location of the centre of the pappus. Using the

observed relationship between pappus angle and the point of minimum u_z (Fig. 2g), a cleaner version of the location of minimum u_z was established for each sample. At this location, u_z profiles across the r direction of the image were plotted (e.g. Fig. S2b) and the following integral calculated (Fig. 2i):

$$\int_0^{D/2} u_z \, r \, dr$$

to establish the extent of the velocity deficit in the wake of the pappus. Integrals were calculated for a fixed 10 mm window around the centre of each sample. This distance was chosen as it corresponds to the smallest observed pappus diameter in the dataset. The flow structure is not well resolved beyond the limit of the vortex (the frame rate is too low to capture the faster flow speeds of the external regions) so this limited the r range for the analysis. Similarly, as flow velocities could not be accurately quantified beyond the z limits of the vortex, the nominal vortex length was determined by obtaining the point beyond the centre of the pappus at which streamwise flow (z direction) reached an arbitrary value of 0.02 m/s. This does not give the actual length of the vortex but gives an indicative value to compare between samples and treatments.

Meteorological data analysis. Hourly meteorological data was obtained from the Integrated Surface Database from the National Centers for Environmental Information (USA). Data for a 30 year period (1987 – 2017) were acquired for each location (Edinburgh (55.950, -3.373), Norwich (52.676, 1.283), Nottingham (52.831, -1.328), Manchester (53.354, -2.275), Exeter (50.734, -3.414)) and filtered according the following criteria: entries were excluded if hourly wind speed, dewpoint or temperature were missing; data were only used from the beginning of April to the end of October in each year; occasional data measured between hours were excluded. Relative humidity was calculated from the dewpoint and temperature. The release height of dandelion seeds was assumed to be 0.35 m according to (4). Wind speeds at this height were calculated by integrating the wind speed over a logarithmic profile following (5) and (6).

Dispersal modelling. The WALD model of wind dispersal was used to predict dandelion seed dispersal distances at varying terminal velocities (7). This is an analytical mechanistic model based on an inverse Gaussian distribution that uses hourly wind speeds and features of vegetation structure to predict dispersal kernels. Vegetation height around dandelions was taken to be 0.17 m, a value obtained from LEDA, a database of Northwest European flora life history traits (8). We assumed surface roughness, friction velocity and turbulent flow to be similar to dispersal of thistle species (short herbaceous vegetation), so used the same values and calculation methods for these parameters as (5). Seed falling velocities for dry and wet conditions were 0.3 and 0.7 m/s respectively, corresponding to the measured values from our drop tests. Dispersal kernels were obtained for each location by selecting a time point at random, calculating the wind speed at dandelion height (as above) and selecting a dispersal dis-

tance according to the probability distribution given by the WALD function. This was repeated for 10,000 simulations for each model run giving an overall dispersal kernel for the weather conditions at that location.

Detachment assays. A modified version of the method in (9) was used to assess detachment of seeds from the capitulum. Tests were conducted in a horizontal, open-circuit wind tunnel. The test section was 1 m long with a rectangular cross-section of 450x400 mm (Fig. 4a). Either 3 days (Fig. 4) or 10-14 days after opening (Fig. S4), samples were placed in the middle of the test section and were subjected to a flow speed of 2 m/s for 30 seconds. Samples were held in place by passing an aluminium rod (rod diameter = 1.5 mm or 3 mm depending on stem diameter) through the hollow stem attached to the capitulum or for older samples, in which the stem had degraded (Fig. S4), were clamped to the rod. Detached seeds were collected in a mesh at the end of the test section (Fig. 4a) and counted. This was repeated for 4, 6, 8 and 10 m/s. After the maximum wind speed, the number of seeds remaining on the capitulum was also counted. Unless otherwise stated, the turbulent intensity was 1.7%. For more turbulent conditions, a grid consisting of 11 equally spaced vertical rods (diameter = 10 mm) was created and placed inside the test section (200 mm downstream of the inlet). This increased turbulence intensity to 9.1%, but the maximum wind speed was reduced slightly to 9.8 m/s and this was used instead of 10 m/s. Wet capitula were treated by placing in the moisture chamber with the humidifier switched on for 1 hour before placing in the wind tunnel.

Data analysis and statistics. Detachment assays were analysed by fitting Kaplan-Meier survival models to the data, with log-rank tests used to compare treatments (R package 'survival'). For falling velocity tests, the following model was fitted to the data: $falling\ velocity \sim cos^{(-2/3)}(pappus\ angle)$ similarly to (10) and dry and wet groups were compared using Student's 2-sample t-test. For PIV data, linear regression models were fit to the data. For the plot of the relationship between C_D and Re, loess regression with a span of 0.8 was used to illustrate the trends in the data.

Bibliography

1. Cathal Cummins, Madeleine Seale, Alice Macente, Daniele Certini, Enrico Mastropaolo, Ignazio Maria Viola, and Naomi Nakayama. A separated vortex ring underlies the flight of the dandelion. *Nature*, 562:414–418, 2018. doi: doi.org/10.1038/s41586-018-0604-2.

2. William Thielicke and Eize J. Stamhuis. PIVlab – towards user-friendly, affordable and accurate digital particle image velocimetry in MATLAB. *Journal of Open Research Software*, 2:e30, 2014. doi: doi.org/10.5334/jors.bl.

3. Jerry Westerweel and Fulvio Scarano. Universal outlier detection for PIV data. *Experiments in Fluids*, 39:1096–1100, 2005. doi: 10.1007/s00348-005-0016-6.

4. Jelle Treep, Monique de Jager, Leandra S Kuiper, Gabriel G Katul, and Merel B Soons. Costs and benefits of non-random seed release for long-distance dispersal in wind-dispersed plant species. *Oikos*, 127:1330–1343, 2018. doi: 10.1111/oik.04430.

5. Olav Skarpaas and Katriona Shea. Dispersal patterns, dispersal mechanisms, and invasion wave speeds for invasive thistles. *The American Naturalist*, 170:421–430, 2007. doi: 10.1086/519854.

6. James M Bullock, Steven M White, Christel Prudhomme, Christine Tansey, Ramón Perea, and Danny A P Hooftman. Modelling spread of British wind-dispersed plants under future wind speeds in a changing climate. *Journal of Ecology*, 100:104–115, 2012. doi: 10.1111/j.1365-2745.2011.01910.x.

7. G G Katul, A Porporato, R Nathan, M Siqueira, M B Soons, D Poggi, H S Horn, and S A Levin. Mechanistic analytical models for long-distance seed dispersal by wind. *The American Naturalist*, 166:368–381, 2005.

8. M Kleyer, R M Bekker, I C Knevel, J P Bakker, K Thompson, M Sonnenschein, Poschlod P, J M van Groenendael, L Klimeš, J Klimešova, S Klotz, G M Rusch, M Hermy, D Adriaens, G Boedeltje, B Bossuyt, A Dannemann, P Endels, L Götzenberger, J G Hodgson, A-K Jackel, I Kühn, D Kunzmann, W A Ozinga, C Römermann, M Stadler, J Schlegelmilch, H J Steendam, O Tackenberg, B Wilmann, J H C Cornelissen, O Eriksson, E Garnier, and B Peco. The LEDA Traitbase : a database of life-history traits of the Northwest European flora. *Journal of Ecology*, 96:1266–1274, 2008. doi: 10.1111/j.1365-2745.2008.01430.x.

9. Eelke Jongejans, Nicholas M Pedatella, Katriona Shea, Olav Skarpaas, and Richard Auhl. Seed release by invasive thistles: the impact of plant and environmental factors. *Proceedings of the Royal Society B*, 274:2457–2464, 2007. doi: 10.1098/rspb.2007.0190.

10. Qing'an Meng, Qianbin Wang, Kaibin Zhao, Pengwei Wang, Peiqing Liu, Huan Liu, and Lei Jiang. Hydroactuated Configuration Alteration of Fibrous Dandelion Pappi: Toward Self-Controllable Transport Behavior. *Advanced Functional Materials*, 26:7378–7385, 2016. doi: 10.1002/adfm.201602596.
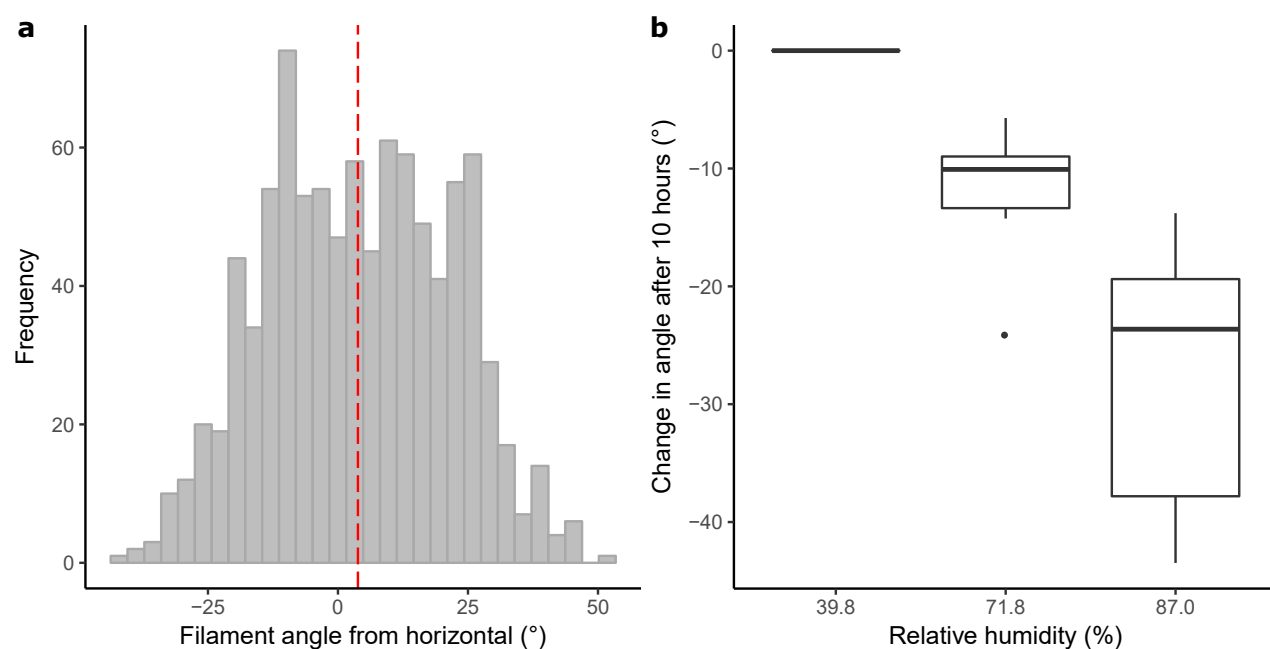
Fig. S1. Supplementary Figure 1. **a** the angle of individual filaments of dandelion pappi. Angle is calculated relative to horizontal in which the dandelion seed beak (see Fig. 1c) forms the vertical axis. N = 10 pappi, n = 932 filaments. Red dashed line indicates the median value. **b** high relative humidity partially closes the dandelion pappus. Change in pappus angle at stable relative humidity (after 10 hours in chamber with saturated salt solutions), n = 7 for 39.8% relative humidity and n = 6 for 71.8% and 87.0% treatments.
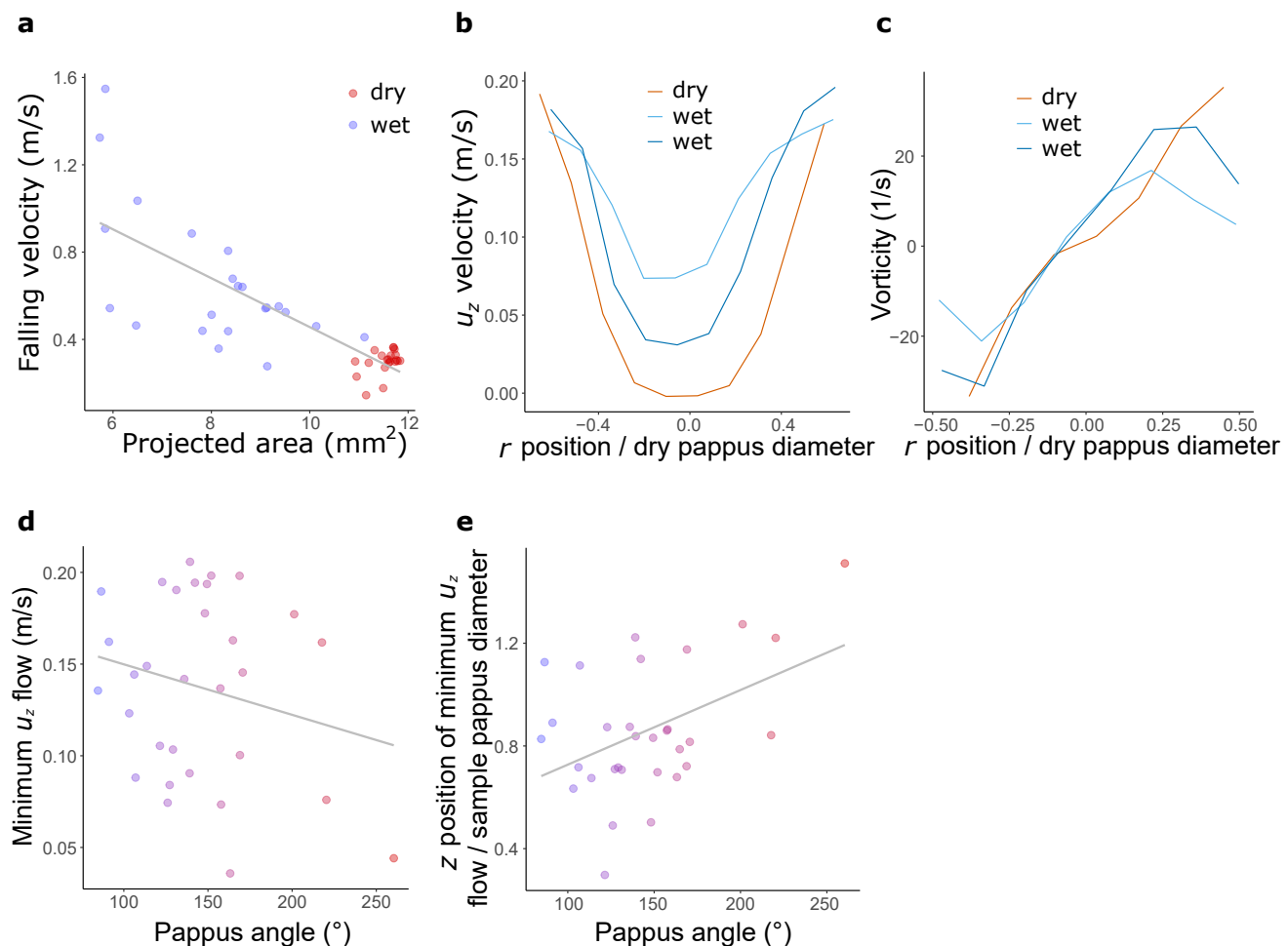
Fig. S2. Supplementary Figure 2. **a** falling velocity reduces as projected area reduces. Projected area calculated using measured pappus angles and assuming filament lengths of 7.41 mm and diameters of 16 μm according to (Cummins et al., 2018). **b** flow velocity along the r axis of vortex images at calculated position of minimal u_z flow. The r position is non-dimensionalized by dividing by the dry pappus diameter for each sample, with 0 indicating the centre of the pappus. Plot for a single sample at 3 different pappus angles, representative of n = 10 samples. **c** vorticity along the r axis of vortex images at calculated position of minimal u_z flow. The r position is non-dimensionalized by dividing by the dry pappus diameter for each sample, with 0 indicating the centre of the pappus. Plot for a single sample at 3 different pappus angles, representative of n = 10 samples. **d** the minimum u_z flow velocity in the separated vortex ring at varying pappus angles. **e** the distance downstream of maximum reverse flow in the separated vortex ring at varying pappus angles. The z position is relative to the sample pappus diameter (i.e. the diameter of the sample at the given pappus angle, rather than in a dry state).
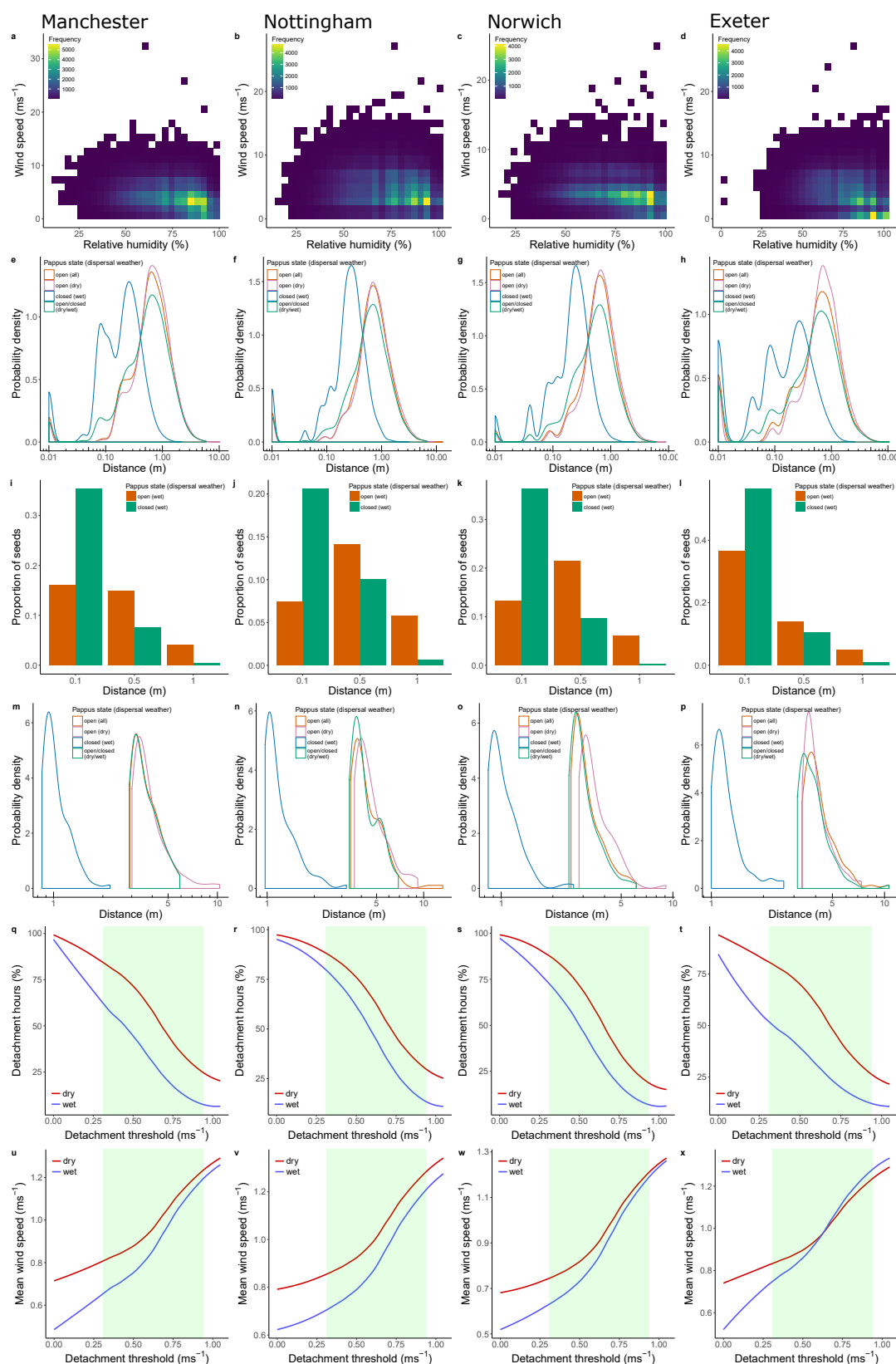
Fig. S3. Supplementary Figure 3. Same plots as Fig.3a-f corresponding to Manchester (**a,e,i,m,q,u**), Nottingham (**b,f,j,n,r,v**), Norwich (**c,g,k,o,s,w**) and Exeter(**d,h,l,p,t,x**).
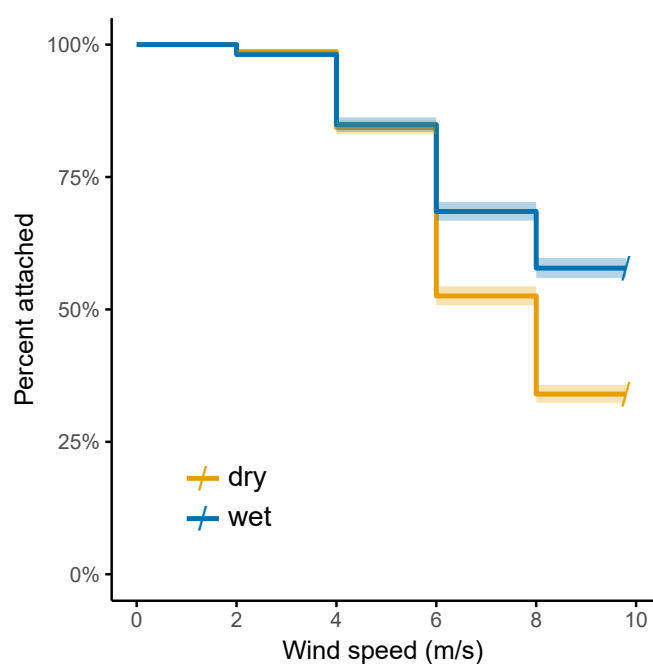
Fig. S4. Supplementary Figure 4. Detachment of dry and wet dandelion seeds from capitula in turbulent flow. Survival plot of percentage of fruits attached to capitula at varying wind speeds with a turbulence intensity of 9.1% in dry and wet conditions, tested 10-14 days after capitula opening, n = 20 capitula per treatment corresponding to 3001 and 2654 seeds for dry and wet conditions respectively, shading indicates s.e.m.